Internal Temperature Distributions of Toner Layer During Flash Fusing Analyzed by a Discrete Particle Model

Teruaki Mitsuya*

Katsuta Research Laboratory, Hitachi Koki Co., Ltd., Hitachinaka, Ibaraki 312 Japan

Kunio Hijikata†

Department of Mechano-Aerospace Engineering, Tokyo Institute of Technology, Ohokayama, Meguro, Tokyo 152 Japan

We propose a discrete model for analyzing a temperature field during a flash fusing. The model is composed of each packed toner particle on a paper surface with assumed spherical shape and discrete coordinates. The contact condition for each particle and paper defines thermal resistance. The advantage of the model is that particle characteristics for the toner layer are considered, and more accurate analysis of the surface and interface toner temperature is possible compared with the previous layered model. First, the discrete particle model is introduced. Then, temperature changes of the toner layer during flash fusing are examined by the discrete particle model and important conditions for obtaining good fixed images are established. The calculated internal temperature in the toner layer shows that the temperatures at the top of the layer are greatly increased and similar for each particle group; however, the temperatures at the bottom of the layer vary significantly for the particle groups. The particle group structured from a smaller number of particles shows a higher bottom temperature. We suggest that to avoid smeared images and to obtain high print quality, the toner layer should be controlled to have small and uniform particle number.

Introduction

In a fusing process in electrophotographic machines, the toner is heated and fused to the substrate paper. With increasingly higher printing speeds, the main subject for study of the fusing process has focused on increasing the interface temperature between toner and paper in a shorter period to obtain sufficient fixing strength. However, modern printing technology forces us to examine the problem of retaining sufficient fixing strength without deterioration of print quality. To achieve good print quality, increase of surface temperature of the toner should be controlled. In addition, the dual and often conflicting requirements of increasing the interface temperature and controlling the surface temperature should be balanced.

The two common types of fixing processes use either radiant or conductive heating called flash fusing[1,2] and heat roll fusing,[3,4] respectively. Flash fusing, for which a xenon flash lamp is used, has the advantage of heat supply to the toner in high-speed printing. However, a disadvantage of flash fusing is that the radiant energy absorbed at the surface of the toner results in a significant surface temperature increase.

Previously, a 1-dimensional, two-layer model composed of the toner and paper layers with respective uniform thermal properties was used to analyze the temperature field during flash fusing.[1,2] These studies were effective for a qualitative comparison of the temperatures in the toner layer. However, because the toner layer is composed of a plurality of toner particles in a perpendicular direction to the paper, the assumption of the uniform properties of the toner layer is not sufficient for the quantitative analysis. More accurate analysis was needed to optimize the surface and interface temperatures of the toner. In this report, the temperatures in the particles are analyzed to reveal more realistic thermal behavior during flash fusing by a model with the toner layer composed of discrete particles called the discrete particle model.

Previous Model and Its Results

Figures 1(a) and 1(b) show the previous 1-dimensional, two-layer model for the temperature analysis and its results.[1] Nonmodified and modified results are shown. Thermophysical properties are modified to correspond with an experimental surface peak temperature of the toner layer in the modified results. Comparing to the experimental result, the peak temperature is much higher in the non-modified case. Input energy is obtained as $1.21\times$ incident energy, in consideration of paper reflection at an uncovered spot with the toner in an imaged area. Regardless of the conditions, the temperatures change more rapidly than the experimental result. The input energy in the calculations may be too great, yielding on unrealistically rapid increase of the surface temperature. Furthermore, although temperature in the experimental result decreases linearly with time, the rate of decrease is different from those of the calculated results.

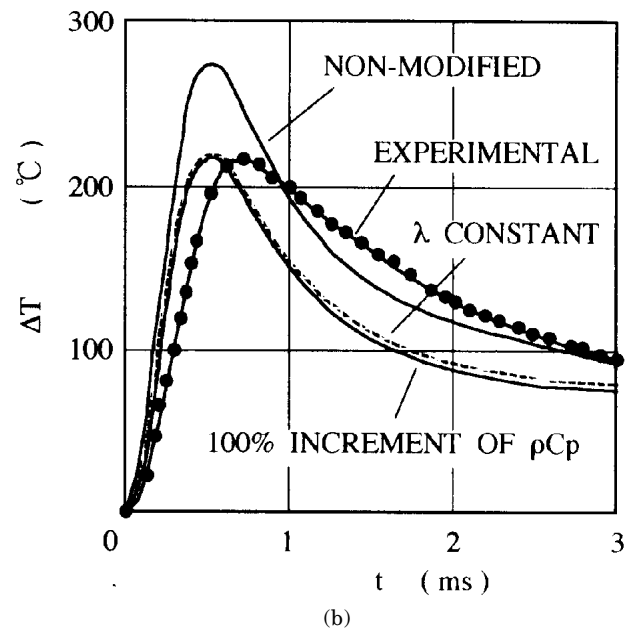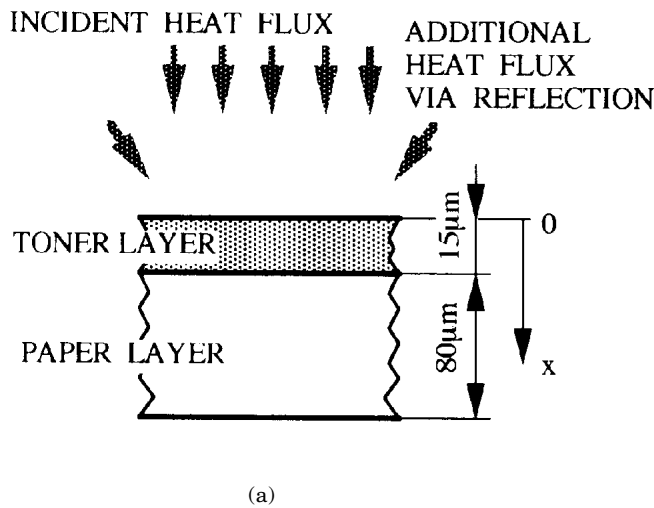A few problems can be found in the previous model. These are:

Figure 1. Previous analysis: (a) model and (b) results.

1. The input energy is absorbed at the surface of the toner layer. The energy absorption distribution at the toner particle surface is not considered.
2. Thermal connections between particle–particle and particle–paper are not considered.
3. Effects of toner layer deformation by melting are not considered.

The difference from the experimental result may be caused by these problems. However, solutions to these problems are limited because experimantal characteristics of the toner layer are not considered in the previous model.

Discrete Particle Model

Model Geometry. Recently, we created a discrete particle model that enables us to consider the characteristics of the toner particle packed bed.

Normally, the toner coverage At/A is lower than 1 (Ref. 5). Therefore, in a microscopic view, the toner layer must consist of the scattered existence of particle groups gathered from particles on the paper. Thermal conduction between particles in the group is via contact points of particle–particle and particle–paper.

Figure 2 shows the model geometry, governing equations, and boundary conditions of the discrete particle model. Spherical-shaped particles that have the same diameters are assumed. Three particle groups are on the paper. Particle packing in the group is assumed to be in a linear pile of 1 to 3 particles in the perpendicular direction to the paper. A differential equation for 1-dimensional thermal conduction is used for each particle and the paper. Area change of the horizontal cross section is considered in the equation for each particle. The heat flux is supplied to the upper half-surface of the top particle in each group and on the paper surface uncovered by the particles. The thermal contact resistance Rh_t is used in boundary conditions at the particle–particle contact points. A combination of the particle–paper thermal contact resistance Rh_p for each particle group and the supplied heat
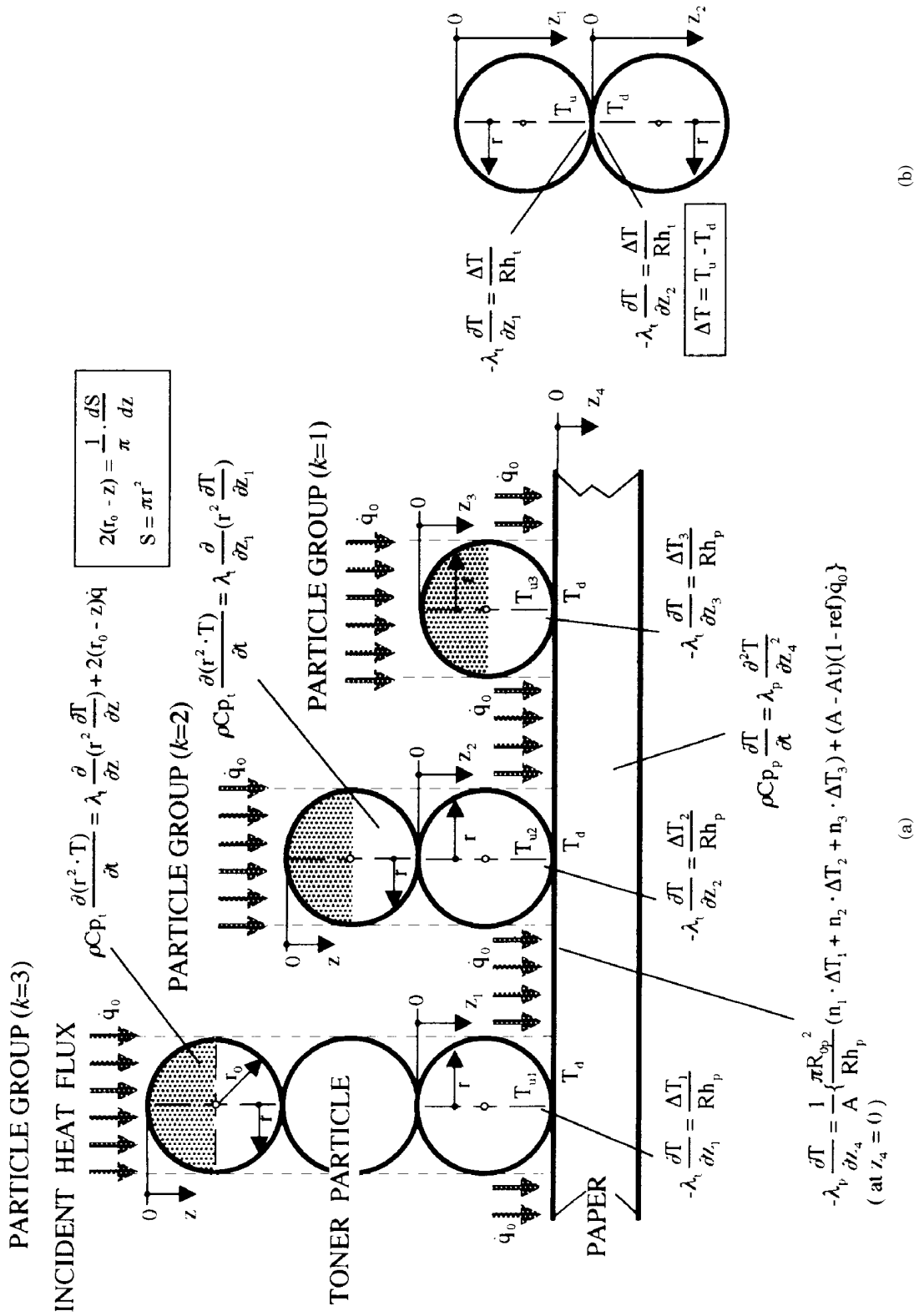
flux is used in the boundary condition at the paper surface. The index number n_k ($k = 1, 2$, and 3) of each particle group and the uncovered paper surface area $A - A_t$ on paper area A are considered in the paper surface boundary condition. The heat flux supplied to the paper decreases from the incident heat flux corresponding to the paper surface reflectivity, *ref*. The thermal contact resistances of Rh_t and Rh_p decrease in the predetermined temperature range at each contact point for consideration of the particle melting deformation.
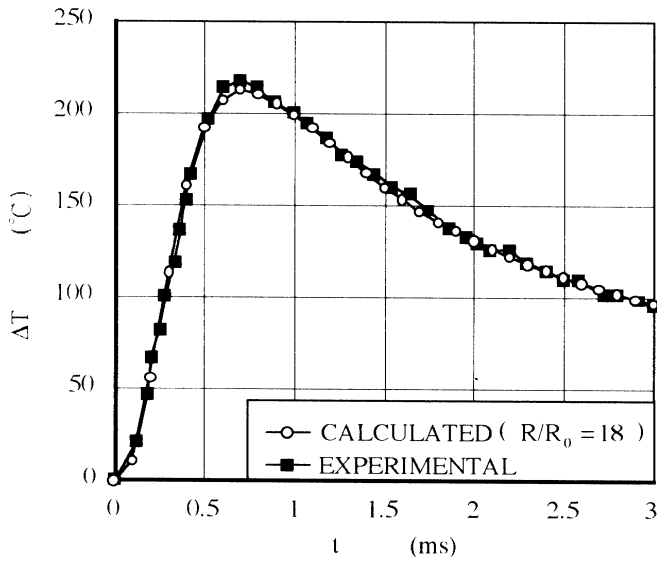
Comparison with Experimental Result. Figure 3 shows the calculated result of the proposed model and the experimental result in the previous work.[1] The calculation is carried out by the finite-difference method. Details are provided below. An infrared radiation thermometer was used for the measurement. The experimental result shows an averaged value for the toner surface and the uncovered paper surface temperatures. For comparison between calculated and experimental temperatures, the calculated result should be arranged by radiation. The averaged temperature T, which is comparable to the experimental result, is given by Eq. 1 using each particle group top-most surface temperature Tt_k, the particle covered area At_k, the paper surface temperature T_p, and the paper area A,

$$\sigma \varepsilon T^4 A = \sigma \varepsilon \Big[T_{t,1}^4 At_1 + T_{t,2}^4 At_2 + T_{t,3}^4 At_3$$
$$+ T_{t,p}^4 \big\{ A - \big(At_1 + At_2 + At_3 \big) \big\} \Big] \tag{1}$$

where σ and ε are the Stefan-Boltzmann constant and toner/paper emissivity. At the wavelength used for measurement (11 µm), toner and paper have equal emissivity of 1.

The calculated result shows excellent correspondence to the experimental result over the whole regime. The discrete particle model has a great advantage of accuracy over the 1-dimensional, two-layer model, as the thermal contact resistance significantly affects the thermal conduction in the toner layer.

Figure 2. Discrete particle model: (a) governing equation, input energy, and particle–paper contact conditions; (b) particle–particle contact condition.

Figure 3. Comparison between calculated and experimental results.

Calculated Conditions. Table I shows the conditions used in the calculation shown in Fig. 3. For comparison, the conditions of the nonmodified result of the previous calculation[1] are also listed.

Particle Diameter and Group Coverage. The particle diameter of 9.6 μm determined from the measured average diameter of unfused toner developed on the paper is used in the present is calculation. This toner is the same as the one examined in the previous temperature measurement.[1] The number of the particles in the group is varied in a range of 1 to 3 and should be dominated by 1 and 2 based on the previously measured average and maximum thickness of the toner layer, which are 15 and 23 μm, respectively.[1] Assuming that the groups of 1 and 2 particles have the same existence numbers and using the previously measured toner coverage ($At/A = 0.72$) and toner layer average thickness,[1] the coverage of each particle group listed in Table I is derived. The measured toner layer average thickness is satisfied by these coverages.

Thermophysical Properties. Thermophysical properties of a solid toner material of thermal conductivity λ_{ts} and ρCp_{ts} must be used in this calculation. The conductivity λ_{ts} is estimated[6] from Eq. 2, using the effective conductivity[1] of toner powder λ_{te}, listed in Table I,

$$\lambda_{ts} = \frac{\rho_{ts}}{\rho_{te}}\lambda_{te}, \qquad (2)$$

where ρ_{ts} and ρ_{te} are solid and effective densities of the toner, which are measured as 1290 and 426 kg/m³, respectively. To derive ρCp_{ts}, the specific heat of solid toner material Cp_{ts} is estimated from the previously measured result obtained by differential scanning colorimetry.[1] The Cp_{ts} averaged above glass transition temperature, $Tg = 60°$, and ρ_{ts} are multiplied for the derivation of ρCp_{ts}.

Contact Point Radius. To derive the thermal contact resistance at the contact point of particle–particle and particle–paper, the contact point radius is needed. The force acting on a particle is needed to derive the radius and is divided into forces from the paper and from other up/down located particles. The force acting on a particle in the particle group with m particles is the total of these forces as shown in Eq. 3,

$$F = \frac{q}{2\varepsilon_0\varepsilon_t}\left\{\sigma + \frac{q}{2\pi}\cdot\sum_{k=1}^{m-1}\left(j_k\cdot\frac{1}{\ell_k^2}\right)\right\}, \qquad (3)$$

where ε_0, ε_t, and q show, respectively, electric permitivity in vacuum, specific permitivity[7] of toner ($\varepsilon_t = 3.61$), and electric charge[8] of a particle ($q = 8 \times 10^{-15}$ C), σ is the surface charge density of paper and is derived from $\sigma = n \cdot q/A$ using the particle number n in the paper area A, and ℓ_k denotes the distance to the up/down located particle k. When the particle is located upward $j_k = 1$ and downward $j_k = -1$. Thus, using Eq. 3, the estimated average forces acting on the particle–particle and particle–paper contact points are 8.6×10^{-9} and 1.8×10^{-8} N, respectively.

Once the contact forces are clarified, Hertz's contact theory[9] can be used for deriving the contact point radius. The derived particle–particle and particle–paper contact point radii R_{0t} and R_{0p} are listed in Table I. In the derivation, Poisson ratios of toner and paper are set at 0.3 and Young's moduli are 2.0×10^9 N/m² for epoxy resin[10] as the toner and 3.9×10^8 N/m² for the paper.[11]

Thermal Contact Resistance. Heat flow passes through very narrow contact points. The thermal resistance occurs at the contact points and significantly affects the toner layer thermal conduction. The thermal resistance can be estimated by using the contact point radius. Figure 4 shows a schematic of the particle–particle contact. Solving a differential equation for the thermal conduction in a point symmetrical geometry using the inner temperature of the upper particle T_u and temperature at contact point T_m, the temperature near the contact point T is obtained by Eq. 4,

$$T = \frac{R}{r}(T_m - T_u) + T_u, \qquad (4)$$

where r denotes distance from the contact point and T_m can be eliminated using the equation for the lower particle temperature obtained using the same procedure. The heat passing through contact point Q obtained by differentiating the T_m erased equation on r is given by Eq. 5,

$$Q = \pi R\lambda_s (T_u - T_d), \qquad (5)$$

where T_d is the inner temperature of the lower particle. Using Eq. 5, the thermal resistance at the particle–particle contact point Rh_t is shown as,

$$Rh_t = (T_u - T_d)\frac{\pi R^2}{Q} = \frac{R}{\lambda_s}. \qquad (6)$$

For the particle–paper contact, the same procedure as for the particle–particle contact can be used. The contact resistance Rh_p is given in Eq. 7,

$$Rh_p = \frac{R(\lambda_s + \lambda_p)}{\lambda_s\lambda_p}, \qquad (7)$$

where λ_p is the thermal conductivity of the paper. The derived thermal resistances Rh_t and Rh_p are listed in Table I.

Contact Point Expansion. Physical estimation of the expanding behavior caused by particle melting is difficult because of the complexity of the phenomenon. However,

TABLE I. Calculated Conditions

		Present	Previous
Particle diameter	D	9.6 µm	Not considered
Particle group coverage	At_1/A	0.29	
	At_2/A	0.29	Not considered
	At_3/A	0.15	
Thermophysical properties	λ_{ts}	0.60 W/(mK)	0.20 W/(mK)
	ρCp_{ts}	1.7×10^6 J/(m³K)	1.4×10^6 J/(m³K)
	λ_p	0.11 W/(mK)	0.11 W/(mK)
	ρCp_p	1.6×10^6 J/(m³K)	1.6×10^6 J/(m³K)
Initial contact point radius and thermal resistance	R_{0t}	2.48×10^{-8} m	
	Rh_t	4.1×10^{-8} m²K/W	Not considered
	R_{0p}	5.60×10^{-8} m	
	Rh_p	6.0×10^{-7} m²K/W	
Contact point radius expansion	R/R_0	18 $(\Delta T > 60°C)$	Not considered
Heat flux correction by paper reflection	$\dot{q}/\dot{q}_0$	1.08	$\dot{q}/\dot{q}_0$ 1.21

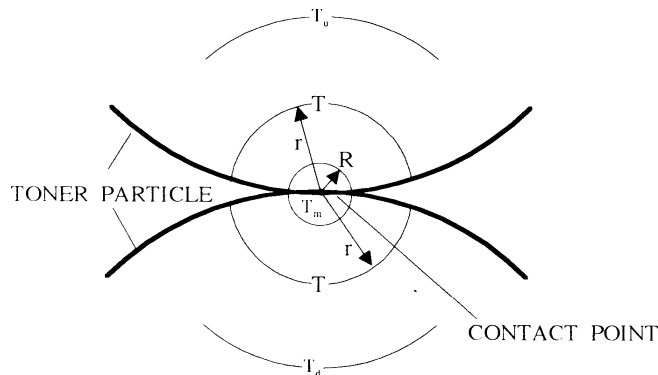

Figure 4. Schematic of particle–particle contact point.

Figure 5. Internal temperature of toner layer.

at least, the contact point must expand as the particle propagation during melting. In the case where the contact point radii remain at their initial values, the authors observed, although not shown in the figures, that the averaged temperature T is no longer comparable to the experimental result above $\Delta T = 60°$. By setting the contact point radius expansion $R/R_0 = 18$ above $\Delta T = 60°$ for each contact point temperature, the excellent correspondence with the experimental result as shown in Fig. 3 is obtained. This clarifies that the effect of the particle deformation by melting is also an indispensable factor and is effective in a temperature range of $\Delta T > 60°$.

Heat Flux Correction. The previously calculated result[1] shows a much faster temperature increase than the experimental result. A reason for this behavior may be that the heat flux may be applied to the toner layer is overestimated. In a temperature range in which the melting effect is negligible, the temperature increase rate may be proportional to the amount of the heat flux to the toner. The temperature range not affected by melting is below $\Delta T = 60°$, as examined in the section on contact point expansion in the present paper. Therefore, in the calculation, the heat flux is set at a value at which the calculated result corresponds with the measured result below $\Delta T = 60°$. The incident heat flux is $\dot{q}_0$ 3.2×10^3 J/m². The heat flux for the toner particle used in this study q is multiplied by correction $\dot{q}/\dot{q}_0$ listed in Table I. This modifica-
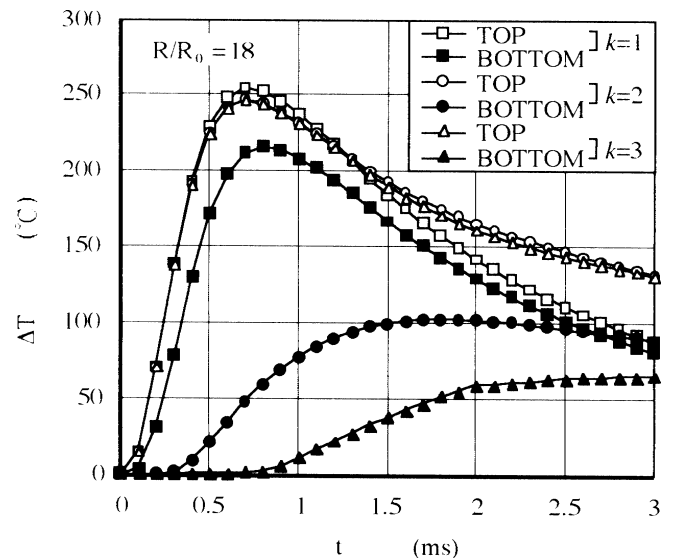
tion is made for the correction by the secondary radiation from the paper reflection at an uncovered spot with the toner in an imaged area.

Internal Temperature Distribution in Toner Layer. Figure 5 shows temperature changes for each particle group ($k = 1$, 2, and 3), at the top and the bottom of the toner deposits, calculated by the discrete particle model. The bottom denotes very close location to the interface with the paper. The top temperatures show large increase, regardless of group. The bottom temperatures vary significantly with the groups. For the groups formed by 1 particle ($k = 1$), the bottom temperature increases significantly and is similiar to its top temperature. For groups formed by 2 and 3 particles ($k = 2, 3$), the bottom temperatures are much lower than for the $k = 1$ group. Particularly, in the $k = 3$ group, the bottom temperature is slightly higher than the temperature affected by melting ($\Delta T > 60°$) and sufficient fixing strength may not be obtained. Actually, because the toner layer is formed of ramdomly distributed particle groups, the bad influence of the $k = 3$ group would appear as a smeared image. The

top temperature should be decreased to obtain high print quality, thereby avoiding significant melting on the particle surface. The counter measurement for this item is possible only for the $k = 1$ particle group. Because this group has a sufficient bottom temperature, the input heat flux can be decreased without deterioration of the fixing strength; then the top temperature decreases. From this result, to avoid smeared images and to obtain high print quality, the toner layer should be controlled to have a smaller and more uniform particle number.

Conclusions

A simulation is conducted for a quantitatively highly accurate temperature field in the toner layer during flash fusing using the discrete particle model, in which the toner particle groups formed by 1 to 3 particles are located on the paper and each particle is connected by thermal contact resistance. Our study involved the following:

1. A discrete particle model is introduced that has excellent correspondence to the experimental result and by which the thermal conduction mechanism and melting parameters can be made clear.
2. The temperatures at the top of the toner deposit are highly increased and similar for each particle group, however, the temperatures at the bottom vary significantly with the particle groups.

3. To avoid smeared images and obtain high print quality, the toner layer should be controlled to have a small and uniform particle number. ▲

References

1. T. Mitsuya, T. Kumasaka and S. Fujiwara, Study of temperature and toner melting conditions during flash fusing, *Opt. Eng.* **30,** (1) 111–116 (1991).
2. H. S. Kocher, Study of heat transfer in toner during flash fusing by means of electrical analog networks, *IEEE Ind. Appl. Soc. Conf. Rec.* **IAS79: 2C,** 34–42 (1979).
3. T. Mitsuya and T. Kumasaka, Heat transfer and toner melting in an electrophotographic fuser system, *J. Imaging Sci. Technol.* **36,** (1) 88–92 (1992).
4. T. Mitsuya K. Masuda and Y. Hori, Measurement of temperature and the flux changes during fixing process in electrophotographic machines, *Trans. ASME J. Eng. Ind.* **118,** 150–154 (1996).
5. C. G. Edmunds and H. S. Kocher, An optical model for fused xerographic images, *IEEE Ind. Appl. Soc. Conf. Rec.* **IAS78:6C,** 197–201 (1978).
6. D. Kunii and J. Smith, Heat transfer characteristics of porous rocks, *AIChE J.* **6,** (1) 71–78 (1960).
7. Tobita and Nakajima, Toner Charge Dependency of Toner Transfer Ratio, *The Society Journal of The Society of Electrophotography of Japan*, **20**(3), 7 (1982).
8. E. A. Eklund, et. al., *IS&T Tenth Int. Congress on Advances in Non-Impact Printing Technologies Proc.* pp 142–146 (1994).
9. S. P. Timoshenko and J. N. Godier, *Theory of Elasticity*, 2nd ed., McGraw-Hill, (1951) pp. 372–377.
10. *The Chemical Handbook: Edition for Application*, Edited by The Chemical Society of Japan, Maruzen (1985), p. 811.
11. Kodaya, et. al., Science of paper manufacturing, Chugai Sangyo Chosaki (1982), p. 658.